

A numerical study of non-perturbative corrections to the Chiral Separation Effect in quenched finite-density QCD

Matthias Pühr* and P. V. Buividovich†

Institute of Theoretical Physics, Regensburg University, 93040 Regensburg, Germany

(Dated: March 25th, 2017)

We demonstrate the non-renormalization of the Chiral Separation Effect (CSE) in quenched finite-density QCD in both confinement and deconfinement phases using a recently developed numerical method which allows, for the first time, to address the transport properties of exactly chiral, dense lattice fermions. This finding suggests that CSE can be used to fix renormalization constants for axial current density. Explaining the suppression of the CSE which we observe for topologically nontrivial gauge field configurations on small lattices, we also argue that CSE vanishes for self-dual non-Abelian fields inside instanton cores.

Anomalous transport phenomena which involve collective motion of chiral fermions are important in many disparate sub-fields of physics ranging from cosmology and astrophysics [1–4] over solid state physics [5–7] to high energy physics and heavy-ion collision experiments [8–11]. Well-known examples of such phenomena are the induction of vector or axial currents along the magnetic field in a dense chiral medium, dubbed the Chiral Magnetic (CME) [8, 12] and the Chiral Separation (CSE) [3, 8, 13, 14] effect, respectively. In particular, for quark-gluon plasma produced in off-central heavy-ion collisions, CSE can locally induce large chirality imbalance [15], and, combined with CME, lead to a novel gapless hydrodynamic excitation - the chiral magnetic wave (CMW) [16].

Within the hydrodynamic approximation, the requirement of positive entropy production together with the Adler-Bell-Jackiw axial anomaly equation fix the transport coefficients describing CME and CSE [17, 18]. However, the hydrodynamic approximation used in [17, 18] might become invalid if the chiral plasma features an infinite correlation length (e.g. due to spontaneous symmetry breaking [19]), or interacts with dynamical Yang-Mills fields [20]. This allows for non-perturbative corrections to CME and CSE. Interactions with dynamic electromagnetic fields also lead to perturbative corrections [21, 22] which we do not consider in this work.

For CSE in QCD matter, which is in the focus of this work, the non-perturbative correction can be expressed in terms of the in-medium amplitude $g_{\pi^0\gamma\gamma}$ of the $\pi^0 \rightarrow \gamma\gamma$ decay [14]:

$$j_i^5 = \sigma_{\text{CSE}} B_i, \quad \sigma_{\text{CSE}} = \sigma_{\text{CSE}}^0 (1 - g_{\pi^0\gamma\gamma}), \quad (1)$$

where j_i^5 is the axial current density and B_i is the external magnetic field. With $g_{\pi^0\gamma\gamma} = 0$ we recover the result $\sigma_{\text{CSE}}^0 = \frac{qN_c\mu}{2\pi^2}$ for N_c species of free chiral fermions (with N_c being the number of colours), which is also expected to be valid in the high-temperature phase with restored chiral symmetry [3, 14, 23].

Within the linear sigma model, an estimate of $g_{\pi^0\gamma\gamma}$ for a medium with spontaneously broken chiral symmetry and at sufficiently small quark chemical potential μ

is $g_{\pi^0\gamma\gamma} = \frac{7\zeta(3)m^2}{4\pi^2 T^2}$, where ζ is the Riemann ζ -function, m is the constituent quark mass and T is the temperature [14]. With realistic values $m \sim 300$ MeV [24] and $T \sim 150$ MeV, which provide a reasonably good description of the chirally broken phase, we get a correction of order of 100% which suppresses the CSE response. Non-perturbative corrections which suppress CSE were also predicted within the Nambu-Jona-Lasinio model [25–27], and within the holographic model of a chiral superfluid with broken Abelian global symmetry [28, 29].

Since non-perturbative corrections to anomalous transport phenomena might significantly modify the predictions of anomalous hydrodynamics, it is important to quantify them in a model-independent way in first-principle lattice QCD simulations. So far a few lattice studies addressed the infrared values of anomalous transport coefficients characterizing the CME [30, 31] and the Chiral Vortical Effect (CVE) [32, 33], and found a very significant suppression of CME and CVE at both low and high temperatures. This is a very puzzling situation, since at least at high temperatures one can expect that the thermodynamic consistency arguments [17, 18] fixing anomalous transport coefficients in hydrodynamic approximation should be valid. Possible reasons for this discrepancy might be the use of naively discretized, non-conserved vector current [30, 31] and energy-momentum tensor [32, 33], and the use of non-chiral Wilson-Dirac fermions in [30, 31]. In summary, this situation clearly calls for more accurate first-principle studies of anomalous transport coefficients which would be free of systematic errors.

In this paper we report on a first-principle lattice study of CSE with finite-density overlap fermions [34], which respect the lattice chiral symmetry at any chemical potential. We use the properly defined lattice counterpart of the continuum axial current density $j_\mu^5 = \bar{\psi}\gamma_5\gamma_\mu\psi$ [35, 36]:

$$j_{x,\mu}^5 = \frac{1}{2}\bar{\psi}(-\gamma_5 K_{x,\mu} + K_{x,\mu}\gamma_5(1 - D_{\text{ov}}))\psi, \quad (2)$$

where $K_{x,\mu} = \frac{\partial D_{\text{ov}}}{\partial \Theta_{x,\mu}}$ is the derivative of the overlap operator D_{ov} over the $U(1)$ lattice gauge field $\Theta_{x,\mu}$. The lattice

axial current (2) transforms covariantly under the lattice chiral symmetry, and is hence protected from renormalization at zero quark mass and can be directly related to the continuum axial current in (1). After some algebra, taking the expectation value on both sides of equation (2) yields

$$\langle j_{x,\mu}^5 \rangle = \text{tr} \left(D_{\text{ov}}^{-1} \frac{\partial D_{\text{ov}}}{\partial \Theta_{x,\mu}} \gamma_5 \right). \quad (3)$$

Technically, the most advanced problem is the calculation of the derivatives $\frac{\partial D_{\text{ov}}}{\partial \Theta_{x,\mu}}$ which enter the definitions of conserved vector and axial currents for overlap fermions. To this end we have developed a special algorithm, described in a separate paper [37].

Lattice QCD with dynamical fermions suffers from a fermionic sign problem at finite quark chemical potential. Moreover, a sign problem seems to be in general unavoidable for gauge theories with dense fermions in a magnetic field, since an external magnetic field breaks time-reversal and/or charge-conjugation symmetries which otherwise ensure the positivity of path integral weight for gauge theories with iso-spin chemical potential or $SU(2)$ or G_2 gauge groups. To avoid the fermionic sign problem, in the present work we neglect the effect of sea quarks and work in the quenched approximation, which was also used for holographic studies of CSE [28, 29]. While arguments from a QCD random matrix model suggest that in the quenched approximation any nonzero chemical potential leads to a vanishing chiral condensate and thus restores chiral symmetry [38], the situation might be different for a magnetized QCD matter, where random matrix theory becomes inapplicable, and non-perturbative corrections to CSE appear due to spontaneous generation of the so-called chiral shift parameter [25–27], rather than chiral condensate.

The $SU(3)$ gauge configurations for our calculations were generated using the tadpole-improved Lüscher–Weisz gauge action [39]. We chose three different lattice setups: $V = L_T \times L_S^3 = 6 \times 18^3$ with $\beta = 8.45$ corresponding to a temperature $T > T_c$ and $V = 14 \times 14^3$ and $V = 8 \times 8^3$ with $\beta = 8.10$ corresponding to $T < T_c$, where L_T and L_S are the temporal and spatial extent of the lattice and $T_c \approx 300$ MeV is the deconfinement transition temperature of the Lüscher–Weisz action [40]. The physical value of the lattice spacing a was determined using results from [41].

For the 14×14^3 and 6×18^3 lattices we generated around 10^3 gauge configurations, from which we randomly picked 100 configurations with topological charge $Q = 0$ [42]. For 6×18^3 we also chose 100 configurations with topological charge $|Q| = 1$, and for 14×14^3 111 with $|Q| = 1$ and 97 with $|Q| = 2$. For the 8×8^3 lattice we generated $5 \cdot 10^3$ configurations, from which three random sets of 200 configurations with $Q = 0$, $|Q| = 1$ and $|Q| = 2$ were selected. We calculated the absolute value of topological charge $|Q| = |n_R - n_L|$ as the number of

zero eigenvalues of the operator $D_{\text{ov}} D_{\text{ov}}^\dagger$, relying on the fact that in practice the overlap operator always has either $n_R = |Q|$ right-handed or $n_L = |Q|$ left-handed zero modes (see e.g. Sec. 7.3.2 in [43]).

Setup	β	8.1	8.1	8.45
	Volume	14×14^3	8×8^3	6×18^3
	Lattice	Phys. Value		
a [fm]	1	0.125	0.125	0.095
V_S [fm ³]	L_S^3	5.4	1.0	5.0
T [MeV]	L_T^{-1}	113	197	346
μ [MeV]	0.050	79	–	–
	0.100	–	158	–
	0.300	474	–	–
	0.040	–	–	83
	0.230	–	–	478
$\frac{qB}{\Phi_B}$ [MeV] ²	$\frac{2\pi}{a^2 L_S^2}$	283 ²	495 ²	289 ²

TABLE I. Simulation parameters

We further introduced a constant, homogeneous external magnetic field following the prescription of [44] with magnetic flux quantum $\Phi_B = 1, 2, 5, 10$ for $V = 14 \times 14^3$ and $V = 6 \times 18^3$ at $Q = 0$, and $\Phi_B = 0, 1, 2, 3, 4$ for $V = 8 \times 8^3$ at all Q . For $V = 6 \times 18^3$ we chose $\Phi_B = 0, 1, 2, 3, 5$ at $|Q| = 1$ and $\Phi_B = 1, 3, 5, 8, 10$ for $V = 14 \times 14^3$ at $|Q| = 1, 2$. For each parameter set, we evaluated the axial current density averaged over the lattice volume for one or two different values of the quark chemical potential μ . The trace in equation (2) was calculated using stochastic estimators with Z_2 -noise. We increased the number of stochastic estimators until the results were stable (see Figs. 1a and 1b for confidence intervals on σ_{CSE} with different numbers of estimators). For configurations with nonzero topological charge we introduced a small quark mass $m_q = 0.001 a^{-1}$ to make the Dirac operator invertible. To demonstrate that finite quark mass has practically no effect on σ_{CSE} , for the 8×8^3 lattice we also considered another value $m_q = 0.002 a^{-1}$. Our simulation parameters are summarised in Table I.

The value of σ_{CSE} is given by the slope of the axial current density as a function of the external magnetic field and can be found by performing a one parameter linear fit to the axial current data (the offset is fixed to zero, since the current has to vanish for $B = 0$). Confidence intervals for σ_{CSE} were computed with the statistical bootstrap, by independently drawing bootstrap samples for every value of Φ_B and fitting the data generated in this way.

First we consider the high-temperature deconfinement phase with $T = 346$ MeV $> T_c$ where chiral symmetry should be at least partially restored as compared to the confinement phase (see e.g. [45, 46] for a discussion of chiral symmetry restoration in quenched QCD). In this case CSE is expected to have no corrections to the free fermion result [3, 14, 23], i.e. $g_{\pi^0\gamma\gamma}(T > T_c) = 0$. To check this

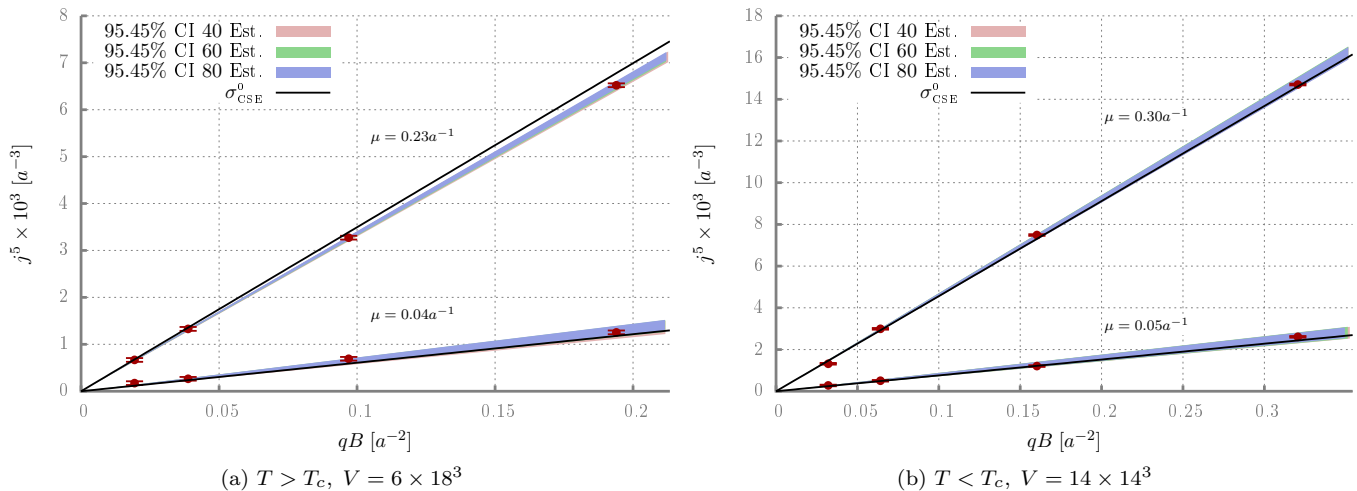


FIG. 1. Axial current density as a function of the magnetic field strength for topological charge $Q = 0$ (red circles with error-bars) at $T > T_c$ (on the left) and $T < T_c$ (on the right). Black lines correspond to the free fermion result σ_{CSE}^0 for both values of the chemical potential. The shaded regions mark the confidence intervals for σ_{CSE} with different numbers of stochastic estimators.

expectation, in Fig. 1a we plot our results for the axial current density for configurations with zero topological charge as a function of qB (data points with error bars). Shaded regions show the bootstrap confidence intervals for different numbers of stochastic estimators which lie on top of each other, hence the error cannot be improved by using more estimators in the trace calculation. We find in general a good agreement with the free fermion result σ_{CSE}^0 , except for the largest values $\Phi_B = 10$ and $\mu = 0.230 a^{-1}$, for which we might see some saturation effect. Therefore we also perform separate fits excluding the data for $\Phi_B = 10$, which show much better agreement with σ_{CSE}^0 . For the larger chemical potential value the signal-to-noise ratio is very good and the relative error of the slope measurement is smaller than 10%. For configurations with $|Q| = 1$ we also find a good agreement with σ_{CSE}^0 within statistical errors. The results for the confidence intervals of σ_{CSE} are summarised in Fig. 2. We conclude that within our statistical errors corrections to CSE are absent in the deconfinement phase of quenched QCD.

We now consider the low-temperature confinement phase at $T < T_c$, where non-perturbative corrections to CSE can be expected [25–29]. In Fig. 1b we plot the axial current density as a function of the magnetic field strength for gauge field configurations with zero topological charge on the 14×14^3 lattice with $T = 113$ MeV and $m_q = 0$. The composition of the plot is the same as for Fig. 1a. The confidence intervals for σ_{CSE} are very small and, again, contain the free fermion result within statistical errors. For the best fits at large chemical potential the relative error of the slope is smaller than 6%. Even for the highest magnetic field strength and the largest chemical

potential we do not see any saturation of the axial current. For configurations with $|Q| = 1$ we again find that σ_{CSE} agrees with the free fermion result σ_{CSE}^0 within confidence intervals (see Figs. 2 and 3). We thus conclude that even in the low-temperature phase of quenched QCD the CSE does not receive any non-perturbative corrections.

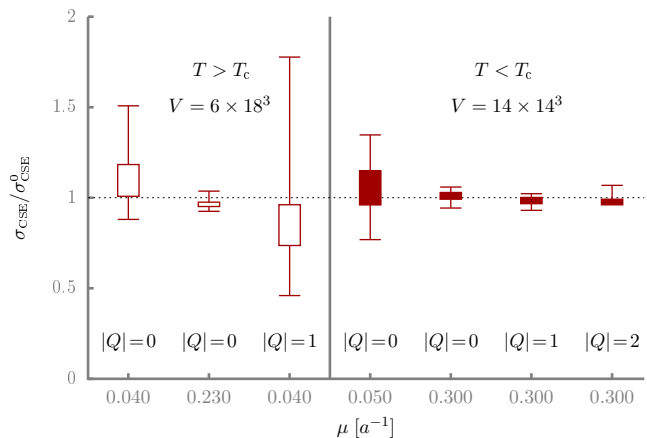


FIG. 2. Confidence intervals for the ratio $\sigma_{\text{CSE}}/\sigma_{\text{CSE}}^0$ for different values of the chemical potential and the topological charge. Boxes and whiskers mark the confidence interval for a fit with all data points and with the largest value of Φ_B excluded, respectively. Filled and open boxes are the results for $T < T_c$ and $T > T_c$, respectively.

At an early stage of this work, we also performed calculations with small lattice volume $V = 8 \times 8^3$ at $\beta = 8.1$ and $\mu = 0.1 a^{-1} = 158$ MeV (see also Table I). While in the zero topological sector we found σ_{CSE} to agree with the free fermion result σ_{CSE}^0 within

statistical errors, which indicates the smallness of finite-volume effects in the $Q = 0$ sector, for configurations with nonzero topological charge we found a rather strong suppression of CSE as well as a non-linear dependence of the axial current on the magnetic field, as illustrated on Fig. 3. We checked that these findings are not finite mass effects by doing calculations with two masses $m_q = 0.001 a^{-1} = 1.6$ MeV and $m_q = 0.002 a^{-1} = 3.2$ MeV, which yield almost identical results. Furthermore, we found that the negative contribution to the axial current which suppresses the CSE comes exclusively from topological modes of the Dirac operator (the eigenvectors which would correspond to zero eigenvalues of the Dirac operator with $m_q = 0$.)

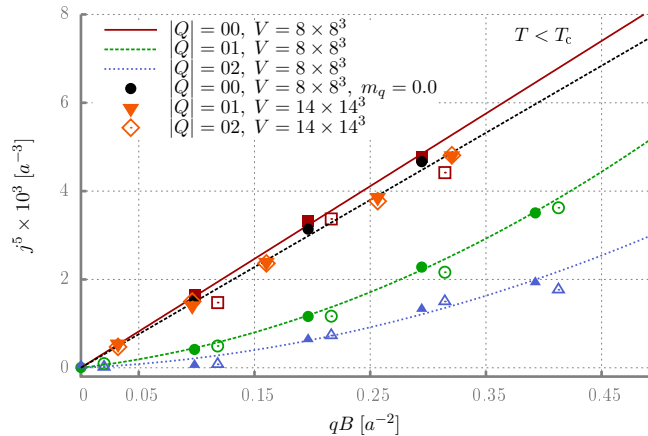


FIG. 3. The axial current in different topological sectors. Filled symbols mark the results for $m_q = 0.001 a^{-1}$, the results for $m_q = 0.002 a^{-1}$ are shifted by $0.02 a^{-2}$ in the qB axis for better visibility and are marked by open symbols. The black dots denote the axial current with $Q = 0$ for vanishing quark mass and the black dashed line corresponds to the free fermion result σ_{CSE}^0 . To guide the eye a linear ($Q = 0$) or second order polynomial ($|Q| > 0$) fit to the data is shown. For comparison we also plot the results for $|Q| > 0$ for the 14×14^3 lattice.

In order to understand the possible origin of the suppression of CSE on topologically nontrivial configurations in small volume, let us consider CSE in a background of constant Euclidean self-dual non-Abelian gauge field, which can be interpreted as a limiting case of very large instanton [47]. For gauge configurations with nonzero topological charge on a small lattice this is a reasonable approximation, as in most cases only a few instantons would fit in a finite box with physical size $L = 8a = 1.0$ fm comparable with the characteristic instanton size [48]. In the gauge where the time-like component of the vector gauge potential depends only on the longitudinal spatial coordinate, thus giving rise to a constant chromo-electric field, eigenstates of the Dirac operator can be labelled by the time-like momentum k_0 . Introducing a finite chemical potential leads to a shift

$k_0 \rightarrow k_0 - i\mu$. However, due to relativistic Landau quantisation in an Euclidean electric field, the dependence of Dirac operator eigenvectors on k_0 reduces to global spatial shifts along the electric field [44, 47], and the corresponding eigenvalues do not depend on k_0 . Upon analytic continuation to complex values $k_0 \rightarrow k_0 - i\mu$, this k_0 independence translates into the independence of volume-averaged axial and vector currents on the chemical potential. Since at zero μ the axial current vanishes, it also vanishes at finite μ . We relegate a more detailed demonstration of this fact to the Supplemental Material. This argument suggests a “porous” spatial distribution of axial current induced due to CSE, which should vanish in regions with self-dual gauge fields. Within the instanton liquid model, these regions can be identified with instanton cores.

To conclude, our numerical study suggests that non-perturbative corrections to the Chiral Separation Effect are either very small (smaller than our statistical errors) or vanishing for finite-density quenched QCD in the thermodynamic limit. By using finite-density overlap fermions [49] with covariant axial current we have eliminated systematic errors due to explicit breaking of chiral symmetry and axial current renormalization. Finite-volume effects also seem to be rather small at least in the zero topology sector. Thus the quenched approximation seems to be the only potentially important source of systematic errors. Indeed, one might argue that we do not find any non-perturbative corrections predicted in [14], since quenched QCD at any nonzero chemical potential is in the chirally symmetric phase with zero chiral condensate [38]. However, the arguments of [38] which are based on random matrix model of QCD might not be directly applicable to QCD in sufficiently strong external magnetic fields, which should introduce certain correlations in the otherwise statistically independent entries of the random matrix which mimics the QCD Dirac operator. Furthermore, calculations within the Nambu-Jona-Lasinio model [25–27] suggest that non-perturbative corrections to CSE are related to spontaneous generation of the so-called chiral shift parameter, which, in contrast to chiral condensate, cannot be described within the random matrix model framework of [38]. Finally, let us recall that also the holographic calculations [28, 29] which do predict non-perturbative corrections to CSE at low temperatures were performed in the quenched approximation (“probe limit” in AdS/QCD terminology).

Of course, these arguments simply illustrate that the non-renormalization of CSE in quenched QCD at both high and low temperatures is a nontrivial result. They do not prohibit non-perturbative corrections which might originate, for example, from the complex phase which the fermion determinant acquires at finite density. Note that external magnetic field renders the fermion determinant complex-valued even for $SU(2)$ or G_2 gauge theories which are otherwise free of sign problem. Since in mass-

less QCD strong oscillations of the determinant phase related to the “Silver Blaze” phenomenon can be expected to set in already at very small density [50, 51], the study of CSE in full QCD with dynamical fermions might be technically very challenging and is out of the scope of this work.

The non-renormalization of CSE at least in quenched QCD can also have a practical application to the calculation of the renormalization constant for the axial current. Namely, the ratio of the CSE-induced axial current calculated with non-chiral lattice fermions and/or some non-covariant discretization of the axial current to the exact result $j_i^5 = \frac{\mu}{2\pi^2} B_i$ yields the multiplicative renormalization constant for the axial current density in this particular discretization.

Finally we note that the precision with which our results reproduce the theoretically expected value $\sigma_{\text{CSE}} = \sigma_{\text{CSE}}^0$ demonstrates that the approach to finite-density overlap fermions developed in [49] and further in [37] provides a reliable tool for first-principle numerical studies of transport properties of dense chiral fermions in lattice QCD.

This work was supported by the S. Kowalevskaja award from the Alexander von Humboldt Foundation. The calculations were performed on “iDataCool” at Regensburg University, on the ITEP cluster in Moscow and on the LRZ cluster in Garching. We acknowledge valuable discussions with G. Bali, A. Dromard and A. Zhitnitsky. MP thanks Rudolf Rödl for helpful comments on the statistical bootstrap.

* Matthias.Puhr@physik.uni-regensburg.de

† Pavel.Buividovich@physik.uni-regensburg.de

- [1] A. Vilenkin, Phys.Rev.D **22**, 3080 (1980), DOI:10.1103/PhysRevD.22.3080.
- [2] H. Tashiro, T. Vachaspati, and A. Vilenkin, Phys.Rev.D **86**, 105033 (2012), arXiv:1206.5549.
- [3] M. A. Metlitski and A. R. Zhitnitsky, Phys.Rev.D **72**, 045011 (2005), arXiv:hep-ph/0505072.
- [4] G. Sigl and N. Leite, J.Cosmol.Astropart.Phys. (2015), arXiv:1507.04983.
- [5] H. J. Kim, K. S. Kim, J. F. Wang, M. Sasaki, N. Satoh, A. Ohnishi, M. Kitaura, M. Yang, and L. Li, Phys.Rev.Lett. **111**, 246603 (2013), arXiv:1307.6990.
- [6] Q. Li, D. E. Kharzeev, C. Zhang, Y. Huang, I. Pletikosic, A. V. Fedorov, R. D. Zhong, J. A. Schneeloch, G. D. Gu, and T. Valla, Nature Phys. **12**, 550 (2016), arXiv:1412.6543.
- [7] G. Basar, D. E. Kharzeev, and H. Yee, Phys.Rev.B **89**, 035142 (2014), arXiv:1305.6338.
- [8] D. Kharzeev and A. Zhitnitsky, Nucl. Phys. A **797**, 67 (2007), arXiv:0706.1026.
- [9] D. E. Kharzeev, L. D. McLerran, and H. J. Warringa, Nucl. Phys. A **803**, 227 (2008), arXiv:0711.0950.
- [10] L. Adamczyk (STAR Collaboration), Phys.Rev.Lett. **113**, 052302 (2014), arXiv:1404.1433.
- [11] D. E. Kharzeev, J. Liao, S. A. Voloshin, and G. Wang, Prog.Part.Nucl.Phys. **88**, 1 (2016), arXiv:1511.04050.
- [12] K. Fukushima, D. E. Kharzeev, and H. J. Warringa, Phys.Rev.D **78**, 074033 (2008), arXiv:0808.3382.
- [13] D. T. Son and A. R. Zhitnitsky, Phys.Rev.D **70**, 074018 (2004), arXiv:hep-ph/0405216.
- [14] G. M. Newman and D. T. Son, Phys.Rev.D **73**, 045006 (2006), arXiv:hep-ph/0510049.
- [15] Y. Burnier, D. E. Kharzeev, J. Liao, and H. Yee, Phys.Rev.Lett. **107**, 052303 (2011), arXiv:1103.1307.
- [16] D. E. Kharzeev and H. Yee, Phys.Rev.D **83**, 085007 (2011), arXiv:1012.6026.
- [17] D. T. Son and P. Surowka, Phys.Rev.Lett. **103**, 191601 (2009), arXiv:0906.5044.
- [18] A. V. Sadofyev and M. V. Isachenkov, Phys.Lett.B **697**, 404 (2011), arXiv:1010.1550.
- [19] P. V. Buividovich, Nucl. Phys. A **925**, 218 (2014), arXiv:1312.1843.
- [20] U. Gursoy and A. Jansen, JHEP **1410**, 92 (2014), arXiv:1407.3282.
- [21] K. Jensen, P. Kovtun, and A. Ritz, JHEP **1310**, 186 (2013), arXiv:1307.3234.
- [22] E. V. Gorbar, V. A. Miransky, I. A. Shovkovy, and X. Wang, Phys.Rev.D **88**, 025025 (2013), arXiv:1304.4606.
- [23] A. Y. Alekseev, V. V. Cheianov, and J. Froehlich, Phys. Rev. Lett. **81**, 3503 (1998), arXiv:cond-mat/9803346.
- [24] L. R. Baboukhadia, V. Elias, and M. D. Scadron, J. Phys. G: Nucl. Part. Phys. **23**, 1065 (1997), arXiv:hep-ph/9708431.
- [25] E. V. Gorbar, V. A. Miransky, and I. A. Shovkovy, Phys.Rev.C **80**, 032801 (2009), arXiv:0904.2164.
- [26] E. V. Gorbar, V. A. Miransky, and I. A. Shovkovy, Phys.Rev.D **83**, 085003 (2011), arXiv:1101.4954.
- [27] E. V. Gorbar, V. A. Miransky, and I. A. Shovkovy, Phys.Lett.B **695**, 354 (2011), arXiv:1009.1656.
- [28] I. Amado, N. Lisker, and A. Yarom, JHEP **06**, 084 (2014), arXiv:1401.5795.
- [29] A. Jimenez-Alba and L. Melgar, JHEP **10**, 120 (2014), arXiv:1404.2434.
- [30] A. Yamamoto, Phys.Rev.Lett. **107**, 031601 (2011), arXiv:1105.0385.
- [31] A. Yamamoto, Phys.Rev.D **84**, 114504 (2011), arXiv:1111.4681.
- [32] V. Braguta, M. N. Chernodub, K. Landsteiner, M. I. Polikarpov, and M. V. Ulybyshev, Phys.Rev.D **88**, 071501 (2013), arXiv:1303.6266.
- [33] V. Braguta, M. N. Chernodub, V. A. Goy, K. Landsteiner, A. V. Molochkov, and M. I. Polikarpov, Phys.Rev.D **89**, 074510 (2014), arXiv:1401.8095.
- [34] J. Bloch and T. Wettig, **97**, 012003 (2006), arXiv:hep-lat/0604020.
- [35] P. Hasenfratz, S. Hauswirth, T. Jörg, F. Niedermayer, and K. Holland, Nucl. Phys. B **643**, 280 (2002), arXiv:hep-lat/0205010.
- [36] Y. Kikukawa and A. Yamada, Nucl. Phys. B **547**, 413 (1999), arXiv:hep-lat/9810024.
- [37] M. Puhr and P. V. Buividovich, Comp.Phys.Comm. **208**, 135 (2016), arXiv:1604.08057.
- [38] M. A. Stephanov, Phys.Rev.Lett. **76**, 4472 (1996), arXiv:hep-lat/9604003.
- [39] M. Lüscher and P. Weisz, Comm. Math. Phys. **97**, 59 (1985), URL <http://projecteuclid.org/euclid.cmp/1103941978>.

- [40] C. Gattringer, P. E. L. Rakow, A. Schaefer, and W. Soeldner, *Phys.Rev.D* **66**, 054502 (2002), arXiv:hep-lat/0202009 .
- [41] C. Gattringer, R. Hoffmann, and S. Schaefer, *Phys.Rev.D* **65**, 094503 (2002), arXiv:hep-lat/0112024 .
- [42] One of the configurations for the parameters $\beta = 8.1$, $\mu = 0.050$ and a magnetic flux of $\Phi_B = 1$ caused a serious breakdown in the Lanczos algorithm when computing the overlap operator. This could not be fixed and we used only the remaining 99 configurations for this parameter set.
- [43] C. Gattringer and C. B. Lang, *Quantum Chromodynamics on the Lattice. An introductory presentation.*, vol. 788 of *Lecture Notes in Physics* (Springer, Berlin Heidelberg, 2010), DOI:10.1007/978-3-642-01850-3.
- [44] M. H. Al-Hashimi and U. Wiese, *Ann.Phys.* **324**, 343 (2009), arXiv:0807.0630 .
- [45] J. Kiskis and R. Narayanan, *Phys.Rev.D* **64**, 117502 (2001), arXiv:hep-lat/0106018 .
- [46] R. G. Edwards, U. M. Heller, J. Kiskis, and R. Narayanan, *Phys.Rev.D* **61**, 074504 (2000), arXiv:hep-lat/9910041 .
- [47] G. Basar, G. V. Dunne, and D. E. Kharzeev, *Phys.Rev.D* **85**, 045026 (2012), arXiv:1112.0532 .
- [48] T. Schaefer and E. Shuryak, *Rev.Mod.Phys.* **70**, 323 (1998), arXiv:hep-ph/9610451 .
- [49] J. Bloch and T. Wettig, *Phys.Rev.Lett.* **97**, 012003 (2006), arXiv:hep-lat/0604020 .
- [50] I. M. Barbour, S. E. Morrison, E. G. Klepfish, J. B. Kogut, and M. Lombardo, *Phys.Rev.D* **56**, 7063 (1997), arXiv:hep-lat/9705038 .
- [51] T. D. Cohen, *Phys.Rev.Lett.* **91**, 222001 (2003), arXiv:hep-ph/0307089 .

Supplemental Material

CHIRAL SEPARATION EFFECT IN TOPOLOGICALLY NONTRIVIAL BACKGROUND OF CONSTANT SELF-DUAL NON-ABELIAN GAUGE FIELD

In order to understand the apparent smallness of the Chiral Separation Effect on topologically nontrivial gauge field configurations, here we consider the simplest topologically nontrivial field configuration with constant and parallel chromo-electric and chromo-magnetic fields of equal strength. If the orientations of both fields in colour space are the same, this configuration is self-dual and has non-zero topological charge proportional to the product of the number of flux quanta of chromo-electric and chromo-magnetic fields. It can be thought of as the instanton of infinitely large size [47].

Since the colour orientations of both chromo-electric and chromo-magnetic fields are the same, they can be simultaneously diagonalized in colour space. After that all fermionic observables reduce to sums over N_c Abelian field configurations with parallel electric and magnetic fields, where magnetic fields also include the $U(1)$ Abelian external magnetic field. Thus in order to demonstrate the vanishing of CSE in such a non-Abelian gauge field background, it is enough to show that it vanishes in the background of constant and parallel Abelian electric and magnetic fields $\vec{E} = \vec{e}_3 E$ and $\vec{B} = \vec{e}_3 B$.

Using the gauge where $A_2 = Bx_1$ and $A_0 = Ex_3$, we can diagonalise the Dirac operator with respect to momenta k_0 and k_2 conjugate to the time variable x_0 and the spatial variable x_2 . With finite quark mass m and quark chemical potential μ , the Dirac operator in such a background can be represented as

$$\mathcal{D} = \gamma_\mu \nabla_\mu + \mu \gamma_0 + m = \begin{pmatrix} m & -iW^- \\ -iW^+ & m \end{pmatrix}, \quad W^\pm = \begin{pmatrix} w_E a_E^\pm & \pm w_B a_B^\dagger \\ \mp w_B a_B & w_E a_E^\mp \end{pmatrix},$$

$$a_E^\pm = \frac{\partial_3}{w_E} \mp \frac{w_E}{2} \left(x_3 - \frac{k_0 - i\mu}{E} \right), \quad a_B = \frac{\partial_1}{w_B} + \frac{w_B}{2} \left(x_1 - \frac{k_2}{B} \right), \quad w_E = \sqrt{2E}, \quad w_B = \sqrt{2B}, \quad (\text{S1})$$

where we have introduced the creation/annihilation operators a_E^\pm and a_B^\dagger, a_B which describe the relativistic Landau quantisation of fermion motion in constant external fields in (x_0, x_3) and (x_1, x_2) planes. These operators satisfy the usual bosonic commutation relations $[a_B, a_B^\dagger] = 1$ and $[a_E^-, a_E^+] = 1$. An interesting new feature is that at finite chemical potential μ the creation and annihilation operators a_E^+ and a_E^- are no longer Hermite conjugate of each other. The reason is that, as one can see from (S1), finite chemical potential results in a complex-valued shift of the potential minimum of a ‘‘harmonic oscillator’’ described by the non-Hermitian ‘‘Hamiltonian’’ $a_E^+ a_E^-$. As a consequence, also the γ_5 -hermiticity of the Dirac operator is lost at finite chemical potential.

The propagator corresponding to the Dirac operator (S1) can be expressed as

$$\mathcal{D}^{-1} = \begin{pmatrix} m(m^2 + W^+ W^-)^{-1} & i(m^2 + W^+ W^-)^{-1} W^+ \\ iW^- (m^2 + W^+ W^-)^{-1} & (m^2 + W^- W^+)^{-1} \end{pmatrix},$$

$$W^+ W^- = \begin{pmatrix} w_E^2 n_E + w_B^2 n_B & 0 \\ 0 & w_E^2 n_E + w_B^2 n_B + w_E^2 + w_B^2 \end{pmatrix}, \quad (\text{S2})$$

where we have introduced the ‘‘electric’’ and ‘‘magnetic’’ number operators $n_E = a_E^+ a_E^-$ and $n_B = a_B^\dagger a_B$, whose eigenvalues label Landau levels in the (x_0, x_3) and (x_1, x_2) planes. This construction is very similar to the one used in [47], with the only difference that a_E^+ and a_E^- are no longer conjugate.

The expectation value of axial current can be now expressed as

$$J_{A3} = \text{tr}(\mathcal{D}^{-1} \gamma_5 \gamma_3) = i \text{tr} \left((W^+ \sigma_3 + \sigma_3 W^-) (m^2 + W^+ W^-)^{-1} \right) =$$

$$= iw_E \text{tr} (a_E^+ + a_E^-) (G(n_E, n_B) - G(n_E + 1, n_B + 1)), \quad (\text{S3})$$

where we have introduced the notation $G(n_E, n_B) = \frac{1}{m^2 + w_E^2 n_E + w_B^2 n_B}$.

The simplest way to proceed now is to express the trace in the above equation in the basis of direct product of eigenstates of bosonic number operators n_E and n_B . While the eigenstates of n_B are the usual harmonic oscillator wave functions corresponding to Landau levels in constant magnetic field, eigenstates of the operator $n_E = a_E^+ a_E^-$

which is non-Hermitian at finite μ deserve a more detailed description. Namely, we first define the left and right “ground state” eigenvectors $\langle L_0|$ and $|R_0\rangle$ of $a_E^+ a_E^-$ which satisfy the equations

$$a_E^- |R_0\rangle = 0, \quad \langle L_0| a_E^+ = 0, \quad \langle L_0| R_0\rangle = \int_{-\infty}^{+\infty} dx_3 \langle L_0| x_3\rangle \langle x_3| R_0\rangle = 1,$$

$$\langle x_3| R_0\rangle = (E/\pi)^{1/4} \exp\left(-\frac{E}{2} \left(x_3 - \frac{k_0 - i\mu}{E}\right)^2\right), \quad \langle L_0| x_3\rangle = (E/\pi)^{1/4} \exp\left(-\frac{E}{2} \left(x_3 - \frac{k_0 - i\mu}{E}\right)^2\right). \quad (\text{S4})$$

We can now define the left and right “excited state” eigenvectors by successively multiplying $|R_0\rangle$ by a_E^+ and $\langle L_0|$ by a_E^- :

$$|R_n\rangle = \frac{(a_E^+)^n}{\sqrt{n!}} |R_0\rangle, \quad \langle L_n| = \langle L_0| \frac{(a_E^-)^n}{\sqrt{n!}}, \quad (\text{S5})$$

Using the identity $a_E^- (a_E^+)^n = (a_E^+)^n a_E^- + n (a_E^+)^{n-1}$ which follows from the commutation relations $[a_E^-, a_E^+] = 1$ and the normalization condition $\langle L_0| R_0\rangle = 1$, it is easy to check that $|R_n\rangle$ and $\langle L_n|$ form the full bi-orthogonal eigenbasis of the operator $a_E^+ a_E^-$, with the eigenvalues n_E corresponding to $|R_n\rangle$ and $\langle L_n|$. It is easy to check that the “wave functions” $\langle x_3| R_n\rangle$ and $\langle L_n| x_3\rangle$ are equal to each other and are simply analytic continuation of the conventional real-valued harmonic oscillator wave functions to the complex-valued position $(k_0 - i\mu)/E$ of the potential minimum. On the other hand, exactly because $\langle x_3| R_0\rangle$ and $\langle L_0| x_3\rangle$ are now complex-valued, $|R_n\rangle$ and $\langle L_n|$ are not complex conjugates of each other.

Using the eigenbasis decomposition of n_B and n_E , we can now rewrite the volume-averaged axial current (S3) as

$$J_{A3} = iw_E \sum_{n_E, n_B} \langle L_n| (a_E^+ + a_E^-) |R_n\rangle (G(n_E, n_B) - G(n_E + 1, n_B + 1)) = 0. \quad (\text{S6})$$

We conclude that the axial current vanishes due to the fact that the matrix element $\langle L_n| (a_E^+ + a_E^-) |R_n\rangle = \sqrt{n_E + 1} \langle L_n| R_{n+1}\rangle + \sqrt{n_E} \langle L_n| R_{n-1}\rangle$ is zero for any n by virtue of the bi-orthogonality relation $\langle L_n| R_m\rangle = \delta_{nm}$. Hence CSE vanishes for such self-dual topologically nontrivial backgrounds of constant non-Abelian gauge fields.
